

ERA-40 Air-Sea Surface Flux Validation

S. RAMOS BUARQUE, G. CANIAUX AND H. GIORDANI

Météo-France, CNRM, 42 av. G. Coriolis, 31057 Toulouse Cedex, France
silvana.buarque@cnrm.meteo.fr

SUMMARY

The European Centre for Medium Range Forecast (ECMWF) 40-year Re-Analysis (ERA-40) air-sea surface flux validation concerns three aspects: (i) intercomparison between earlier re-analysis, (ii) comparison of ERA-40 with in-situ experiments, (iii) comparison of ocean global model response forced by ERA-40 and ERA-15 fluxes and (iv) evaluation of ERA-40 and ERA-15 spin-up.

In the first, ERA-40 global averaged heat flux was compared with ECMWF Re-Analysis 15-year (ERA-15), NCEP/NCAR 40-year and NASA/DAO 15-year. ERA-40 shows smaller global imbalances in net air-sea surface heat fluxes than other re-analyses. Spatial and temporal correlations between air-sea surface heat fluxes of ERA-40 and NCEP/NCAR were examined. Results indicate that ERA-40 latent heat and solar radiation are slightly larger and spatially well correlated to those of NCEP/NCAR. ERA-40 sensible heat and thermal radiation are spatially badly correlated to those of NCEP/NCAR. Bias of sensible heat has no global trends. Generally ERA-40 thermal radiation is smaller than those of NCEP/NCAR. Correlation between interannual anomalies of heat fluxes from ERA-40 and NCEP/NCAR was examined. Interannual anomalies of sensible heat, solar radiation and net heat flux are particularly badly correlated in North Hemisphere.

Validation of heat and momentum fluxes was performed by comparison with in-situ fluxes estimates from five research cruises: POMME, EQUALANT99, FETCH, CATCH-FASTEX and SEMAPHORE. Generally ERA-40 wind stress and latent heat are larger than in-situ experiments. Sensible heat trends are not clear. ERA-40 turbulent flux and downward solar radiation are well correlated with in-situ experiments in mean and high latitudes, however, downward solar radiation shows RMS superior to 50% of averages. ERA-40 averaged downward thermal radiation is similar to observations.

In the third, ERA-40 forcing was compared to those of ERA-15 in term of ocean global model response. ERA-40 is warmer than ERA-15 particularly in central eastern Pacific and western Atlantic. Stronger cold bias is observed at west of Central America and reaches locally 3°C. Warm biases are smaller and spreader than negative biases. ERA-40 mixed layer is shallower on subtropical gyre of the South Pacific and deeper in eastern Pacific than ERA-15.

Finally, in support of oceanographic interests (MERSEA¹, MERCATOR, MFSTEP²), ERA-40 and ERA-15 short-range forecasts was analysed as a function of spin-up, i.e. initial increase (or decrease) of model outputs with forecast length. ERA-40 spin-ups have been generally smaller than those in ERA-15 have. Latent heat fluxes globally increase as a function of the distance from the initialisation time and levels off after 24 hours. This behaviour is due particularly to tropical regions. Sensible and radiative flux spin-up remain constant after 6 hours. Generally, 0-6 hr forecast is nearest to observations.

1. Introduction

Started in autumn 2000, the basic part of the European Centre for Medium Range Forecast (ECMWF) 40-year Re-Analysis (ERA-40) project (Uppala et al., 2000) is finished. Three main assimilation streams can be identified: the first or priority production period from 1989 onwards (Stream 1); the second from mid-1957 to mid-1972 (Stream 2) and the last from mid-1972 to 1985 (Stream 3). Additional assimilation streams and short reruns were necessary due to technical problems or problems with satellite radiance tuning. A final version of the reanalysis products has been

¹ Marine Environment and Security for the European Area

² Mediterranean Ocean Forecasting System: Towards Environmental Predictions

created from all of streams. Instructions about the final version and archive features can be found at http://www.ecmwf.int/research/era/Data_Services/.

The simultaneously production of ERA-40 streams imposed constraints in temporal validation because this mode of production originate temporal discontinuities. Thus, validation of ERA-40 air-sea surface fluxes is assessed from different temporal periods. This report summarises the main results of the validation.

2. Comparison with earlier Re-analysis

ERA-40 air-sea surface heat fluxes were compared with earlier re-analyses: (i) ECMWF Re-Analysis 15-year from December 1978 to February 1994 (ERA-15) (Gibson et al., 1999); (ii) the NCEP/NCAR 40-year analysis from 1948 (Kistler et al., 2001; Kalnay et al., 1996); (iii) the NASA/DAO 15-year analysis from March 1980 (Schubert et al., 1993). Table 1 summarises the main differences between re-analyses.

Table 1. Mainly characteristics of data assimilation system.

ANALYSE	ERA-40	ERA-15 (1979–1993)	NCEP/NCAR (1948-2000)	NASA/DAO (1980-1993)
SPATIAL RESOLUTION	Spectral T159 resolution with 60 vertical hybrid levels.	Spectral T106 resolution with 31 vertical hybrid levels.	Spectral T62 resolution with 28 “sigma” vertical levels.	Latitude-Longitude grid (91×144) with 20 “sigma” vertical levels.
ASSIMILATION MODE	Three-dimensional variational (3D-VAR) analysis with 6 hour cycling.	Statistical Optimum Interpolation (OI) analysis with 6 hour cycling.	Three-dimensional variational (3D-VAR) analysis in spectral space with 6 hour cycling.	Statistical Optimum Interpolation (OI) analysis with 6 hour cycling.

Each component of the net air-sea surface heat flux was evaluated at global scale for 1987-90 and compared to those reviewed by Taylor (2001) for 1981-92 (Table 2). As in the open-literature (White, 2001; Beljaars and Källberg, 2001) ECMWF air-sea heat fluxes are computed from 12-24 hr forecast while NCEP/NCAR and NASA/DAO from 0-6 hr forecast. ERA-40 and ERA-15 regular mesh is of 1.5° and those of NCEP/NCAR is of 1.875°. NASA/DAO has an irregular mesh of 2.5° by 2°. The Net Ocean Surface Flux (NOSF) is given by the sum of turbulent and radiative fluxes. Positive fluxes correspond to a gain for the ocean. Radiative fluxes are the sum of the upward and downward fluxes. ERA-15, NCEP/NCAR and NASA/DAO show comparable heat fluxes for both periods with values for 1981-92 generally larger than those for 1987-90. Intercomparison of re-analysis for 1987-90 shows smallest NOSF for ERA-40. ERA-40 latent heat remains equal to those of ERA-15. ERA-40 sensible heat and thermal radiation respectively increases and decreases compared to those of ERA-15. The improved ERA-40 global balance would be due primarily to ERA-40 solar radiation diminution compared to others re-analysis.

Table 2. Global means of air-sea surface heat fluxes: SLHF (Latent Heat), SSHF (Sensible Heat), SSR (Solar Radiation), STR (Thermal Radiation) and NOSF (Net Heat Flux) in W/m².

Global Means	ERA-40	ERA-15		NCEP/NCAR 40-year		NASA/DAO (GEOS1)	
	1987-90	1987-90	1981-92	1987-90	1981-92	1987-90	1981-92
SLHF	-78	-78	-103	-73.2	-93	-62.1	-80
SSHF	-9.7	-9	-9.8	-7.3	-10.9	-13.5	-10.6
SSR	+135.9	+138.5	+160	+139	+166	+163.7	+198
STR	-47.3	-48.9	-50.6	-54.7	-56.4	-69.6	-67.9
NOSF	+1.3	+2.5	-3.4	+3.8	+5.6	18.5	+39.5

Figure 1 shows linear regression coefficients of spatial correlation between seasonal averaged air-sea surface heat fluxes from ERA-40 and NCEP/NCAR from 1987 to 1990. Both reanalysis was interpolated from their original grid towards a regular grid of 5.625° mesh. In linear regression calculation ERA-40 is on the x-axis. Calculation of regressions coefficients take into account real air-sea surface fluxes variability, i.e. x-axis varies from negative to positive values. The slopes of sensible heat are mainly superior to unity and depend upon the season with an increasing from spring towards winter. This result is opposite to the previous one (Table 2) showing that sensible heat of ERA-40 is globally smaller than those of NCEP/NCAR. Spatial correlation remains modest between 0.7 and 0.9. ERA-40 latent heat is well correlated to those of NCEP/NCAR. For all seasons, ERA-40 latent heat is slightly larger than those of NCEP/NCAR. Solar radiation from ERA-40 and NCEP/NCAR spatially correlate well with each other for all seasons. However, slopes of the order of 0.9 indicate that ERA-40 solar radiation is generally larger than those of NCEP/NCAR. This result is also opposite to the previously global averaged solar radiation comparison. ERA-40 thermal radiation is badly correlated to those of NCEP/NCAR with correlation coefficients varying from 0.4 to 0.6. Results from intercomparison of re-analysis (Table 2) and spatial correlations (Figure 1) show that ERA-40 and NCEP/NCAR has quite different sensible heat and thermal radiation.

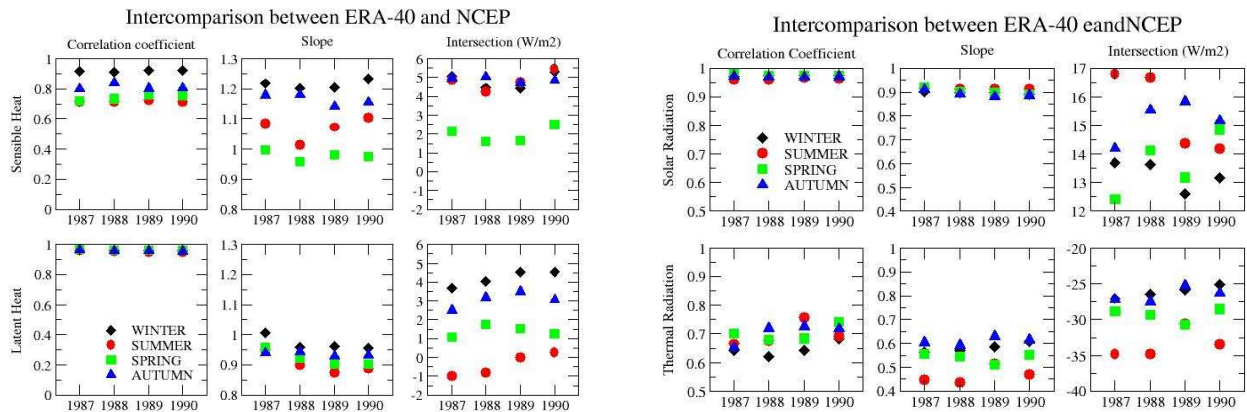


Figure 1. Seasonal regressions of heat flux components between ERA-40 and NCEP/NCAR where ERA-40 is the y-axis.

Temporal correlations between ERA-40 and NCEP/NCAR annual averaged heat fluxes are examined for three assimilation streams over three bands of latitude (Table 3). ECMWF air-sea heat fluxes are computed from 0-6 hr forecast while NCEP/NCAR from 0-3 hr forecast. ERA-40 annual averaged latent heat is generally larger than those of NCEP/NCAR. The correlation maximum is observed in Tropics. From 1973 up to now, latent heat correlation is mainly inferior to 30% in North and South Hemisphere (respectively NH and SH). For 1958-72, latent heat correlation is largely larger than for 1973-2001 and of the order of 70%. The large difference of correlation coefficient for 1973-2001 from those for 1958-72 suggests that both reanalysis are significantly different in the assimilation of satellite data. Note also that the largest lag between ERA-40 and NCEP/NCAR latent heat is observed in SH for all streams. Sensible heat shows mainly positive bias (ERA-40 loses less energy than NCEP/NCAR) and the correlation varies from 30 to 90%. For all streams solar radiation has smallest correlations in the tropics. Generally ERA-40 solar radiation remain larger than those of NCEP/NCAR especially in SH. ERA-40 thermal radiation is inferior to those of NCEP/NCAR. Correlations are maximum in SH and NH for 1989-2001 but in Tropical region this period corresponds to weak correlation. Annual averaged net heat flux (NOSF) for both reanalysis are quite different. ERA-40 and NCEP/NCAR are better correlated in the Tropical region.

Table 3. Temporal statistics of air-sea surface heat fluxes annual mean between ERA-40 and NCEP/NCAR in W/m^2 for three assimilation streams over three bands of latitude.

Periods	Parameters	60°N to 20°N			20°N to 20°S			20°S to 60°S		
		ERA-40	NCEP	Cor	ERA-40	NCEP	Cor	ERA-40	NCEP	Cor
1989-2001	SLHF	-93,9	-93,6	31	-126,5	-126,4	59	-80,5	-68,4	22
	SSHF	-18,3	-20,2	43	-10,6	-12,1	62	-12,2	-11,2	32
	SSR	153,5	157,0	43	202,0	204,5	14	148,6	141,9	76
	STR	-53,2	-59,7	66	-48,0	-54,5	34	-48,1	-57,5	78
	NOSF	-11,9	-16,5	30	16,8	11,5	85	7,9	4,8	15
1973-1988	SLHF	-92,1	-90,9	-5	-130,3	-122,6	32	-78,9	-66,6	-14
	SSHF	-17,9	-20,0	64	-10,2	-10,9	45	-12,2	-11,1	90
	SSR	153,3	157,5	76	205,2	204,5	31	147,8	144,2	-63
	STR	-53,0	-60,2	16	-50,3	-54,3	67	-48,6	-59,2	20
	NOSF	-9,8	-13,6	-14	14,4	16,6	60	8,1	7,3	31
1958-1972	SLHF	-93,1	-93,8	67	-134,2	-129,8	71	-81,7	-71,1	82
	SSHF	-17,1	-20,7	48	-10,4	-12,5	41	-12,8	-14,0	53
	SSR	156,6	157,1	-47	211,0	201,9	-3	148,1	146,1	38
	STR	-54,6	-60,7	-32	-53,4	-54,6	66	-49,3	-61,6	39
	NOSF	-8,1	-18,1	47	13,1	5,0	64	4,2	-0,5	83

The climatology of ERA-40 and NCEP/NCAR heat fluxes was obtained from annual means averaged over 1958-2001 for three bands of latitude. ERA-40 and NCEP/NCAR interannual anomalies were calculated from their respective climatology. Table 4 shows correlations between ERA-40 and NCEP/NCAR interannual anomalies of heat fluxes. Results show interannual correlations inferior to 70% with a minimum in NH. Interannual anomalies of sensible heat, solar radiation and net heat flux are particularly badly correlated in NH. This results given a new source of investigations of oceanic (by forcing ocean models) and atmospheric modes of oscillation.

Table 4. Correlation between ERA-40 and NCEP/NCAR interannual anomalies of heat fluxes: SLHF (Latent Heat), SSHF (Sensible Heat), SSR (Solar Radiation), STR (Thermal Radiation) and NOSF (Net Heat Flux). The climatology of ERA-40 and NCEP/NCAR heat fluxes was obtained from annual means averaged over 1958-2001 for the three bands of latitude.

Period	Parameters	60°N to 20°N	20°N to 20°S	20°S to 60°S
1958-2001	SLHF	43,2	48,8	39,2
	SSHF	6,8	42,8	60,5
	SSR	-1,3	-54,4	-22,9
	STR	39,6	29,7	70,0
	NOSF	-1,5	46,7	60,4

3. Validation by comparison with experiments

Comparison of ERA-40 air-sea surface fluxes with in-situ estimates includes five research cruises: (i) POMME (two IOPs between February to April 2001) in North Atlantic (15°-21°W; 45°-38°N); (ii) EQUALANT99 (42 days since July, 12 to August 1999) which took place from Salvador de Bahia (Brazil) to Abidjan (Ivory Coast) (0°-40°W; 10°N-15°S); (iii) FETCH (from March, 13 to April, 15 1998) in the Mediterranean sea (3°-6.5°E; 42°-43.5°N) (Dupuis, 1996; Hauser et al., 2001); (iv) CATCH-FASTEX (from January, 08 to March, 04 1997) in the Newfoundland Basin (53°-38°N; 28°-44.5°W) (Eymard et al., 1999) and (v) SEMAPHORE (IOP between October, 07 to November, 15 1993) in Southeast of the Azores (36.3°-33°N; 26.3°-22°W) (Giordani, 1998; Eymard et al., 1996). Full description of these experiments and methods used to derive heat and momentum fluxes can be found in Weill et al. (2003).

Air-sea surface turbulent fluxes were obtained using the Inertial Dissipative Method (IDM) (ALBATROS database: <http://dataserv.cetp.ipsl.fr/FLUX/>) and bulk parameterisations. In bulk parameterisations, the neutral transfer coefficients at 10 m height (drag coefficient C_{dn} , and vapour and heat exchange coefficients, C_{en} and C_{hn}) are computed with Smith (1988). Airflow distortion was taken into account for EQUALANT99 (Brut, 2002) and FETCH.

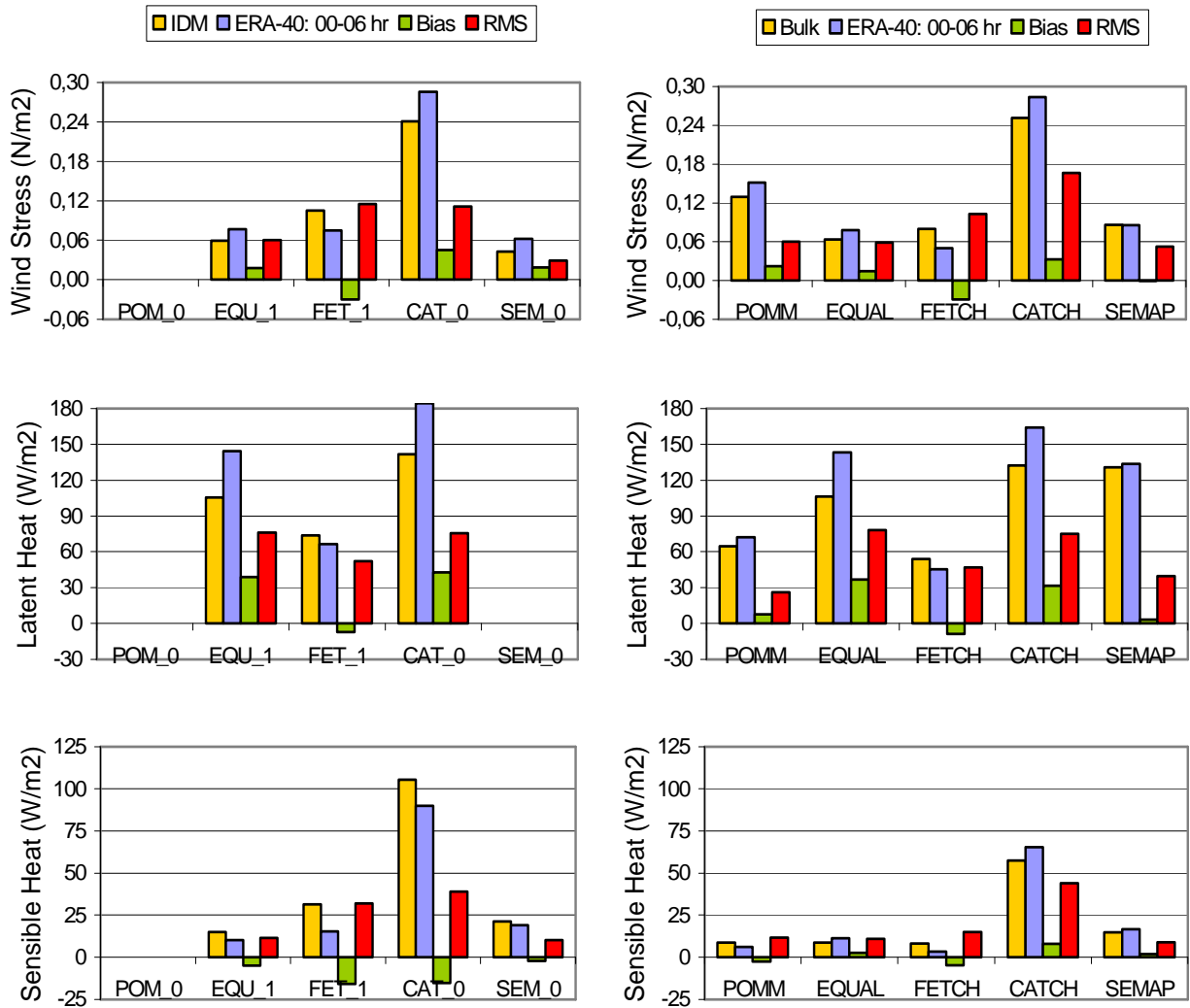


Figure 2. From top to bottom statistics (average, bias and RMS) of wind stress, latent and sensible heat for POMME, EQUALANT, FETCH, CATCH and SEMAPHORE. On the left, comparison between ERA-40 0-6 h forecast and IDM fluxes. On the right, comparison between ERA-40 0-6 h forecast and bulk fluxes.

Turbulent fluxes from both IDM and bulk parameterisation were compared to ERA-40 0-6 hr forecast (Figure 2). In-situ averaged wind stress and latent heat are slightly underestimated by bulk parameterisation in FETCH while in EQUALANT99 and CATCH they are similar. Bias between ERA-40 and observations are similar for both IDM and bulk parameterisation. This result allows concluding from that ERA-40 wind stress and latent heat are larger than observations. Sensible heat shows opposite bias for IDM and bulk parameterisation. This may be partially due to weak number of points used in averages from IDM. Whatever, the RMS is generally as large as averages showing that there is much uncertainty about sensible heat. Correlations between ERA-40 and observations are also examined (Figure 3). ERA-40 turbulent fluxes are well correlated with observations for POMME, CATCH and SEMAPHORE (high latitudes) while for EQUALANT99 (tropics) correlation has not statistical sense. This last result is not agree with those obtained previously when EQUALANT99 fluxes was compared to those of ECMWF operational model which showed

correlation coefficient of 0.75 and 0.45 respectively for latent and sensible heat fluxes (G. Caniaux, personal communication).

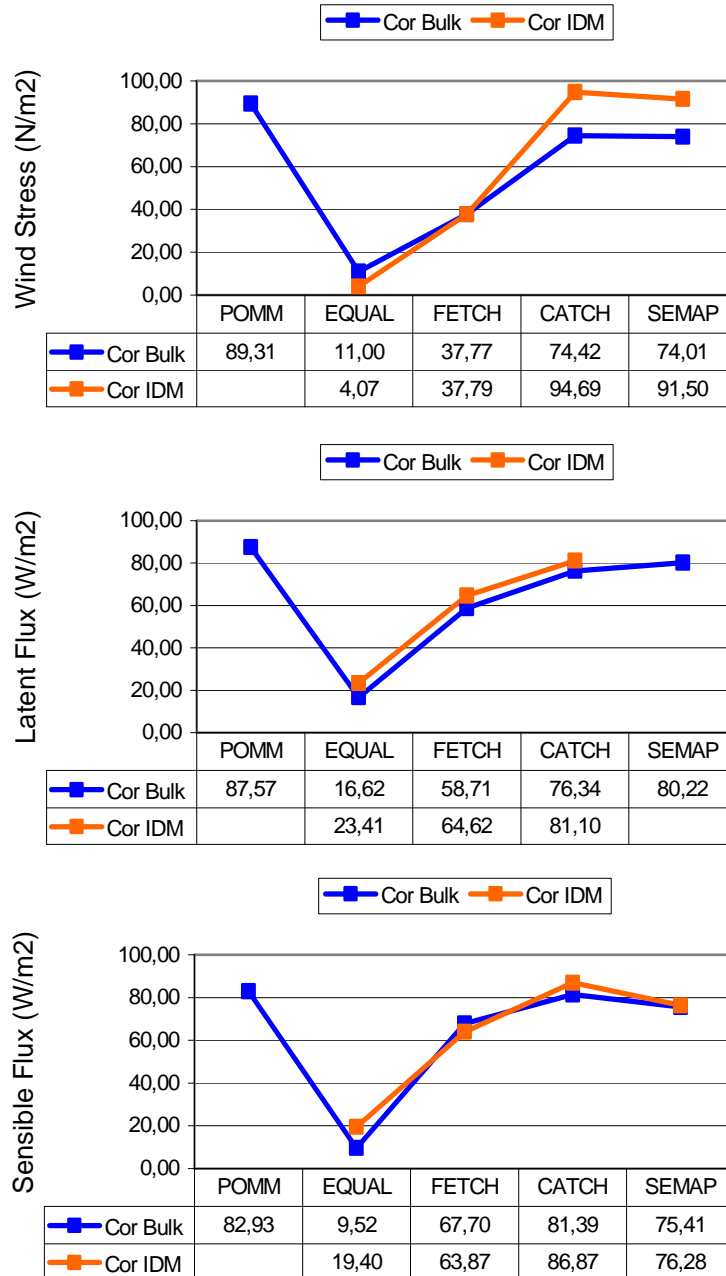


Figure 3. From top to bottom correlation of ERA-40 0-6 h forecast with IDM and bulk fluxes for wind stress, latent and sensible heat.

In-situ downward solar and thermal radiation was also compared to ERA-40 0-6 h forecast (Figure 4). For FETCH CATCH and SEMAPHORE, ERA-40 downward solar radiation is well correlated with observations but the signal of bias varies and the RMS remains superior to 50% of averages. The worse correlation is observed for EQUALANT99 as well for downward solar as downward thermal radiation; however, downward thermal radiation has very small bias and RMS. In the same way, SEMAPHORE shows similar averaged downward thermal radiation from ERA-40 and observation with badly correlation. As for turbulent fluxes, radiative fluxes correlations between

EQUALANT99 and ERA-40 is not agreed with correlations obtained between EQUALANT99 and ECMWF operational model, which is of 0.75 and 0.89 for solar and thermal radiation respectively. ECMWF operational model has a mesh of 40 km while ERA-40 mesh is almost four times larger. ERA-40 was compared to observations at his nearest mesh because this method showed largest correlations compared to those interpolating several points weighted by distance. However, ERA-40 mesh may be too loose when fluxes vary strongly. Indeed, two trajectories of EQUALANT99 are meridian. This may explain in part the small correlations founded in the comparison of ERA-40 with EQUALANT99.

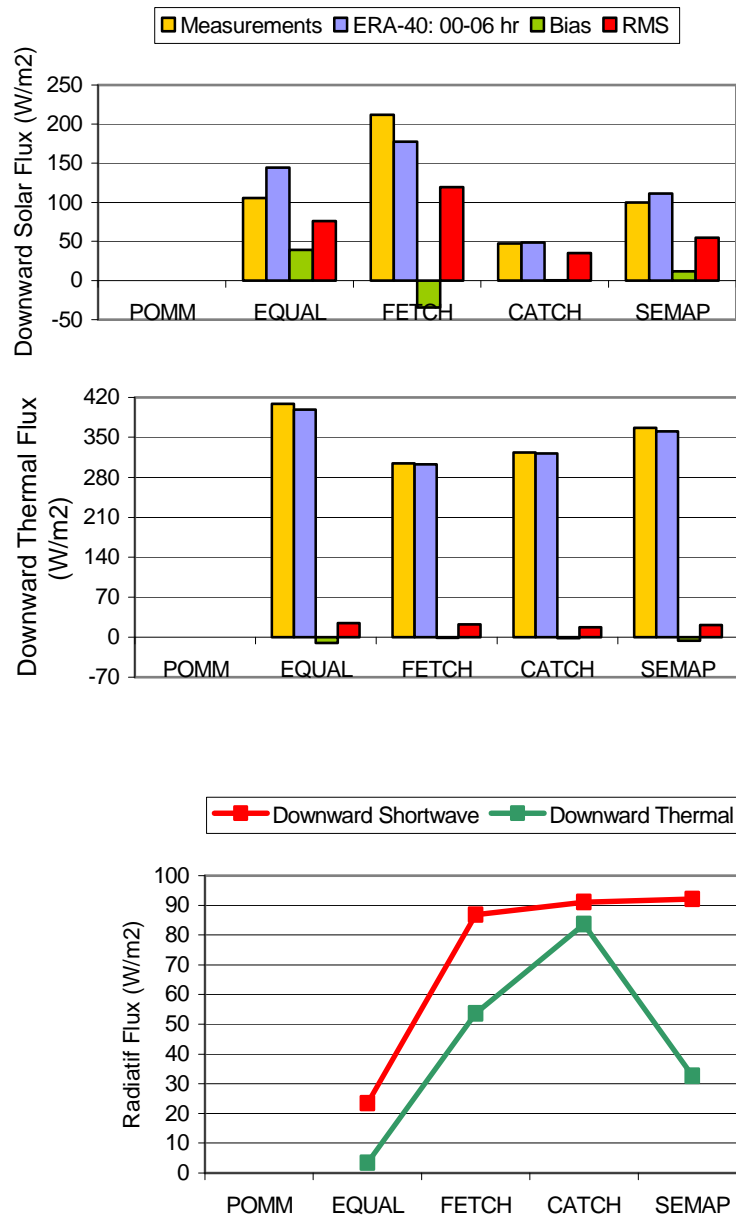


Figure 4. From top to bottom statistics (average, bias and RMS) of downward solar and thermal radiation and correlation ERA-40 0-6 h forecast with observations.

4. Evaluating fluxes in the upper ocean

ERA-40 and ERA-15 fluxes were used to force the Ocean General Circulation Model (OGCM) ORCA 2 degrees, version 8.2 (Madec et al., 1999). Impacts of both reanalysis on oceanic simulations are investigated for 12-24 hours forecast. ORCA2 was forced by sea-surface wind stress and heat fluxes averaged over 1-day period. Sea Surface Temperature (SST) and Mixed Layer Depth (MLD) were evaluated from 5-year integration corresponding to the period from 1989 to 1993.

4.1 The ORCA 2 degrees model

ORCA 2 degrees (ORCA2) is a version of the primitive equation model of ocean circulation OPA (Océan PArallélisé). A rigid lid is assumed at the sea surface. The horizontal mesh is orthogonal and curvilinear on the sphere (Figure 4, top). The grid has two poles in northern hemisphere used to overcome North Pole singularity (Madec and Imbard, 1996). Meridian grid spacing is increased near the equator to improve the equatorial dynamics. The time step is equal to 1h36'. Surface heat and momentum fluxes are provided by the re-analysis, interpolated onto the ocean model grid mesh and updated at each time step. In this forced mode, a feedback term is added to the specified heat flux (Barnier, 1998):

$$Q=Q_0+\frac{dQ}{dT}(SST_{MOD}-SST_{OBS}) \quad 3.1$$

Q_0 is the heat flux prescribed from the re-analysis, SST_{OBS} is the 7-day Reynolds-Smith Sea Surface Temperature (Reynolds and Smith, 1994), SST_{MOD} is the model SST and dQ/dT is a negative feedback coefficient usually taken equal to $-40W/m^2/^{\circ}K$ (Madec and Delecluse, 1997). The difference between SST_{MOD} and SST_{OBS} is called relaxed term. MLD computation is based on a density criterion:

$$\rho(mld)=\rho(0)+\Delta\rho(\Delta T=0.5^{\circ}C) \quad 3.2$$

$\rho(mld)$ and $\rho(0)$ are the salt-water densities in the mixed layer and $\Delta\rho$ correspond to density variation related to temperature difference of $0.5^{\circ}C$ from the surface. MLD is the level having density equal to $\rho(mld)$. For more details see Monterey and Levitus (1997).

4.2 ORCA2 validation

On Figure 5, mean state of SST for the period 1989-93 is compared with *IGOSS nmc Reyn_SmithOIV1* climatology averaged from 1950 to 1979 (<http://ingrid.ldeo.columbia.edu>). The climatology uses blended data from ship, buoy and Reynolds-Smith (1994) bias-corrected satellite observations. The mean state of the SST is generally in good agreement with the climatology. Fronts are well located and oriented. Both simulated and observed SST range from 20° to $30^{\circ}C$ between $20^{\circ}S$ and $20^{\circ}N$. Surface currents distribution and its coherence with MLD are examined (Figure 6). North and south equatorial currents are realistic as well as the east shallow tongue related to them. Circular patterns as Kuroshio and California current, which are respectively strong and weak, correspond respectively to deep and shallow MLD. East Australian Current and Subtropical Gyre are also well represented.

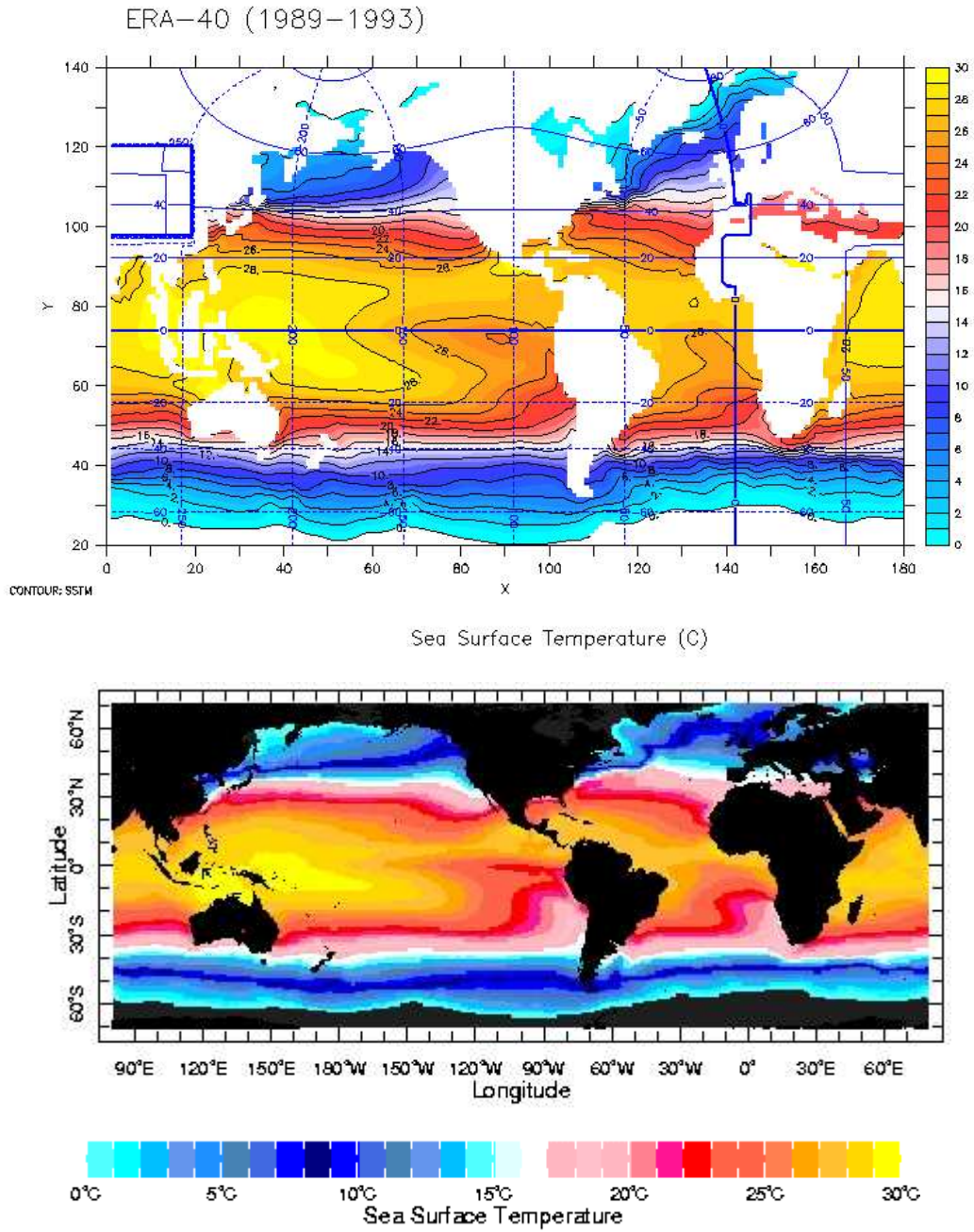


Figure 5. Mean state of Sea Surface Temperature (SST) from ORCA2 for the period 1989-93; ORCA2's grid is superimposed to SST (top). SST from *IGOSS nmc Reyn_SmithOlV* climatology for the period 1950-79 (bottom).

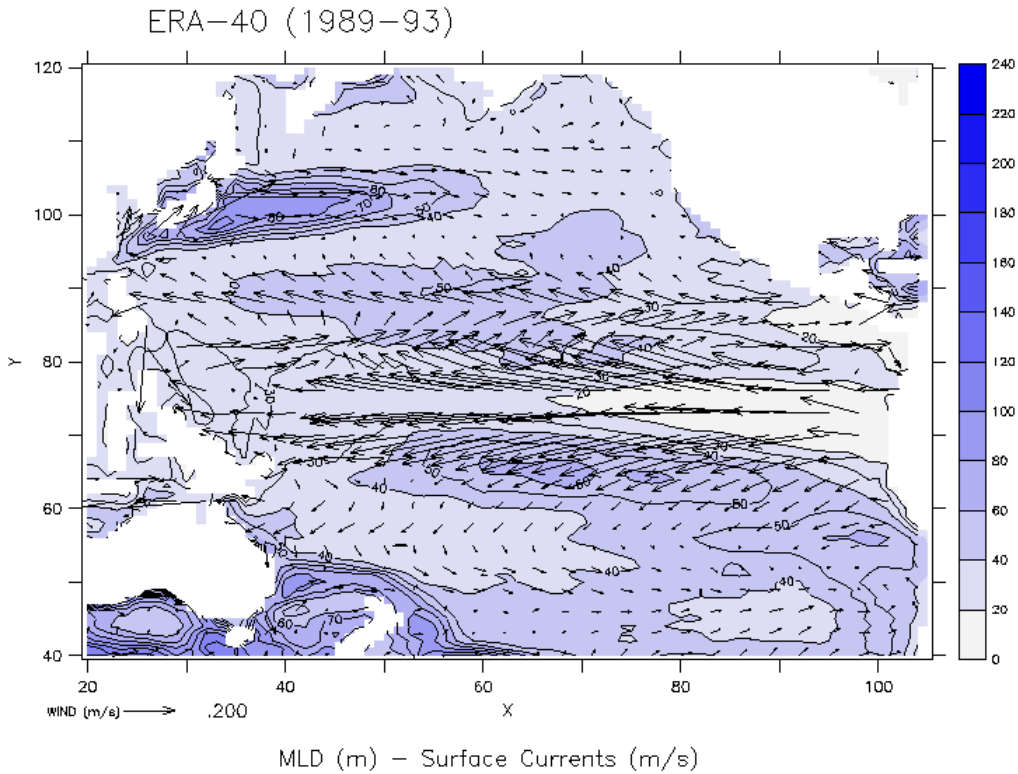


Figure 6. Mean state of surface currents and Mixed Layer Depth (MLD) for the period 1989-93 from ORCA2 in Pacific.

4.3 ERA-40 against ERA-15 in Upper Ocean

Figure 7.a shows global field of SST bias between ERA-40 and ERA-15 averaged from May to October (MJJASO). This period correspond to months showing globally largest differences. Generally, in NH both re-analysis give similar SST forecast. Between the Tropics, ERA-40 is warmer than ERA-15 in eastern Pacific and western Atlantic and Indian Oceans. In SH, the central eastern Pacific is mainly touched by strong warm bias. Stronger cold bias is observed at west of Central America and reaches locally 3°C. Warm biases are smaller and spreader than negative biases Figures 7.b and 7.c show respectively SST and relaxed term evolutions in western Tropical Atlantic (warm bias); Figures 7.d and 7.e show the same parameters in the west coast of Central America (cold bias). Western Tropical Atlantic shows bias of the order of 0.5°C which persist in time; this behaviour are observed generally for regions showing warm bias as eastern Pacific or Northwest Australia off. Both regions show phased SST evolution but the relaxed term is not phased at west of Central America, where the mixed layer is shallow. Concerning MLD, the period from May to October (MJJASO) correspond also to largest bias (Figure 8.a). On subtropical gyre of the South Pacific (10°N-10°S; 85°-125°E), ERA-40 is shallower than ERA-15 during August-September but wind stress evolutions of both reanalysis remain similar (Figures 8.b and 8.c). Conversely, in eastern Atlantic, where the MLD is shallow, ERA-40 is significantly deeper than ERA-15 and the wind stress remain stronger (Figures 8.d and 8.e)

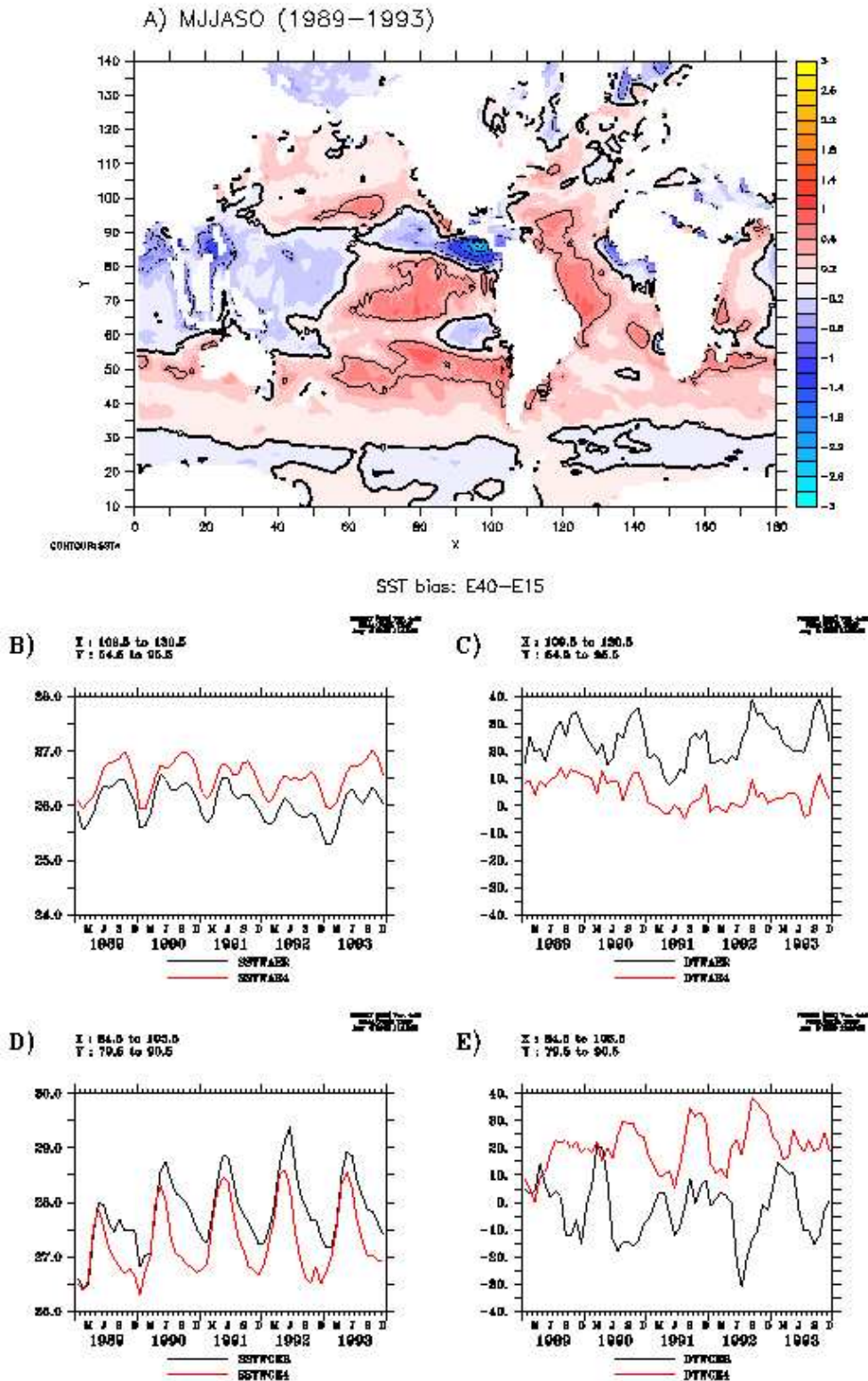


Figure 7. (a) SST bias between ERA-40 and ERA-15 averaged from May to October (MJJASO). Comparison of ERA-40 (red line) to ERA-15 (black line) forcing evolutions: (b) SST and (c) relaxation term in western Tropical Atlantic; (d) SST and (e) relaxation term in the west coast of Central America.

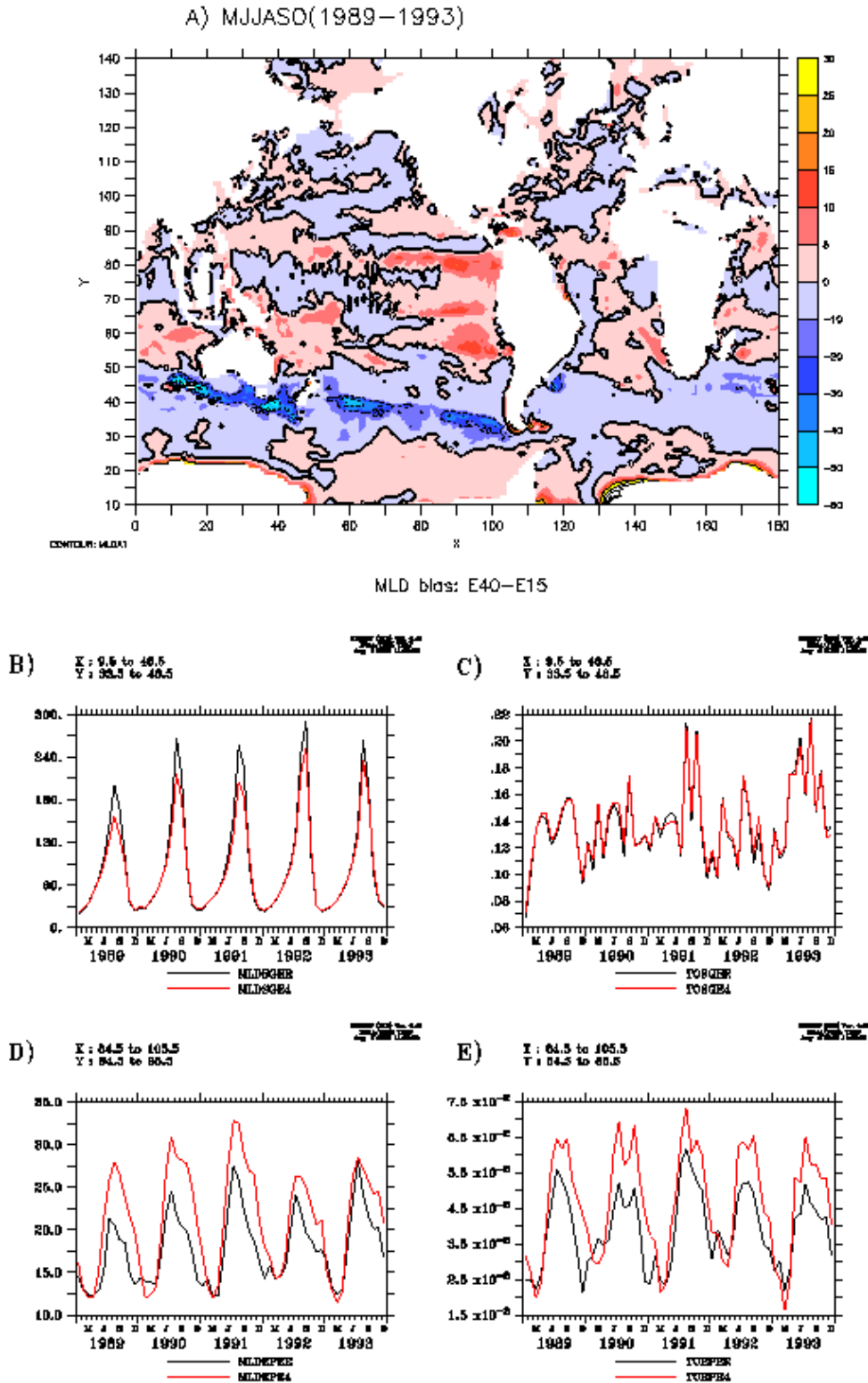


Figure 8. (a) MLD bias between ERA-40 and ERA-15 averaged from May to October (MJJASO). Comparison of ERA-40 (red line) to ERA-15 (black line) forcing evolutions: (b) MLD and (c) wind stress on Subtropical gyre (10°N-10°S; 85°-125°E); (d) MLD and (e) wind stress in Gulf of Guinea (15°W-10°E; 5°S-10°N).

5. Evaluation of heat flux spin-ups

During the first time steps over model integration, surface fluxes depend on imbalances between the initial conditions and the atmosphere consistent with the forecast model's physics and dynamics (White and Saha, 1999; Giordani and Planton, 2000). This phase is called the spin-up period and corresponds to the initial increase (or decrease) of model outputs with forecast length. ERA-40 and ERA-15 short-range forecast spin-up of air-sea surface fluxes was evaluated (Ramos Buarque et al., 2002 and 2003). In order to compare ERA-40 to ERA-15, the study was restricted to those years covered by both re-analysis at the time that the study was undertaken: the period 1989-93. However, this period encloses the Mount Pinatubo eruption (July 1991) and its impact on air-sea fluxes are examined. The clearest impact of eruption on air-sea fluxes is shown by solar radiation. In ERA-40, zonal averaged solar radiation remains unchanged from 1989 to 1993, while in ERA-15 its change globally eight month after the Mount Pinatubo eruption (during March-April-June 1992, not shown) and remains unchanged. Thus, the study was newly made to the period: 1989-91. Results show that qualitative conclusions remain unchanged but local spin-up diminishes ($\approx 1 \text{ W/m}^2$ of global averaged latent heat during the JJA). This shows that it is not necessary to have many years to describe the model behaviour and consequently the evaluation was carried out for the period 1989-91. Spin-up was evaluated at global, large (over bands of latitudes) and regional scales for each component of the heat flux. Impacts of seasonal cycle on spin-up were also considered.

Results showed that radiative fluxes spin-ups were found to be weaker than 10% with a time of stability of the order of 6 hours at all spatial scales. Conversely, turbulent heat flux spin-ups were found to be much larger than those of radiative fluxes. If in terms of percentages, radiative flux spin-ups are much weaker than those of turbulent fluxes; it is larger in terms of magnitude. This means that all fluxes spin-ups can be considered as affecting net surface heat budget. On a global scale, latent heat flux spin-up levels off after 24 hours. Analysis on large scales has shown that this behaviour is due to a major contribution of tropical latitudes whereas beyond 30° North and South, spin-up had stabilized by around 6 hours. Sensible heat flux spin-up stabilize as soon as 6 hours on a global scale. At large scales there are a strong dispersion around the global value. Finally, the regional analysis confirmed the global and large scales results but showed that some seasonal modulations appear on the sensible heat flux at tropical latitudes.

Intercomparison between ERA-40 and ERA-15 showed that ERA-40 spin-ups are weaker than in ERA-15 and always stabilize whereas those in ERA-15 are largely chaotic. In terms of oceanic mixed layer predictability, these two points are crucial. This shows that ERA-40 air-sea fluxes are physically more consistent with the atmospheric parameters than those in ERA-15 are. Order of magnitude of air-sea surface fluxes short-range forecast spin-up has shown that this question is important when the proposal is to compare model-to-model or in-situ data to model outputs. This question also rises when the purpose is to constrain ocean models. For instance, Bonekamp et al. (1999) have shown that the solely thermodynamic forcing is able to trigger the ocean Antarctic Circumpolar Wave mode. Thus, in support of oceanographic interests, spin-up was analysed by running ocean model.

6.1 ERA-40 spin-up evaluation by running ocean model

The sensitivity of ocean model to ERA-40 air-sea fluxes spin-up was also examined. Figure 9.a shows global field of ERA-40 SST bias between 0-6 and 24-36 hours forecast averaged from May to October (MJJASO). This pattern is quite similar to this from November to April (NDJFMA). Globally, bias remain inferior or equal to 0.25°C except in eastern tropical Atlantic and central eastern tropical Pacific. In eastern Atlantic bias is positive (0-6 hr is colder than 24-36 hr forecast) and can exceed locally 1°C ; averaged SST evolution shows that averaged bias appear during February-

March-April and July-August-September (perceptible on Figure 9.b). In central eastern tropical Pacific 0-6 hr is warmer than 24-36 hr forecast with systematic averaged bias of the order of 0.5°C (bias can exceed locally 1.5°C); averaged bias remain almost constant in time.

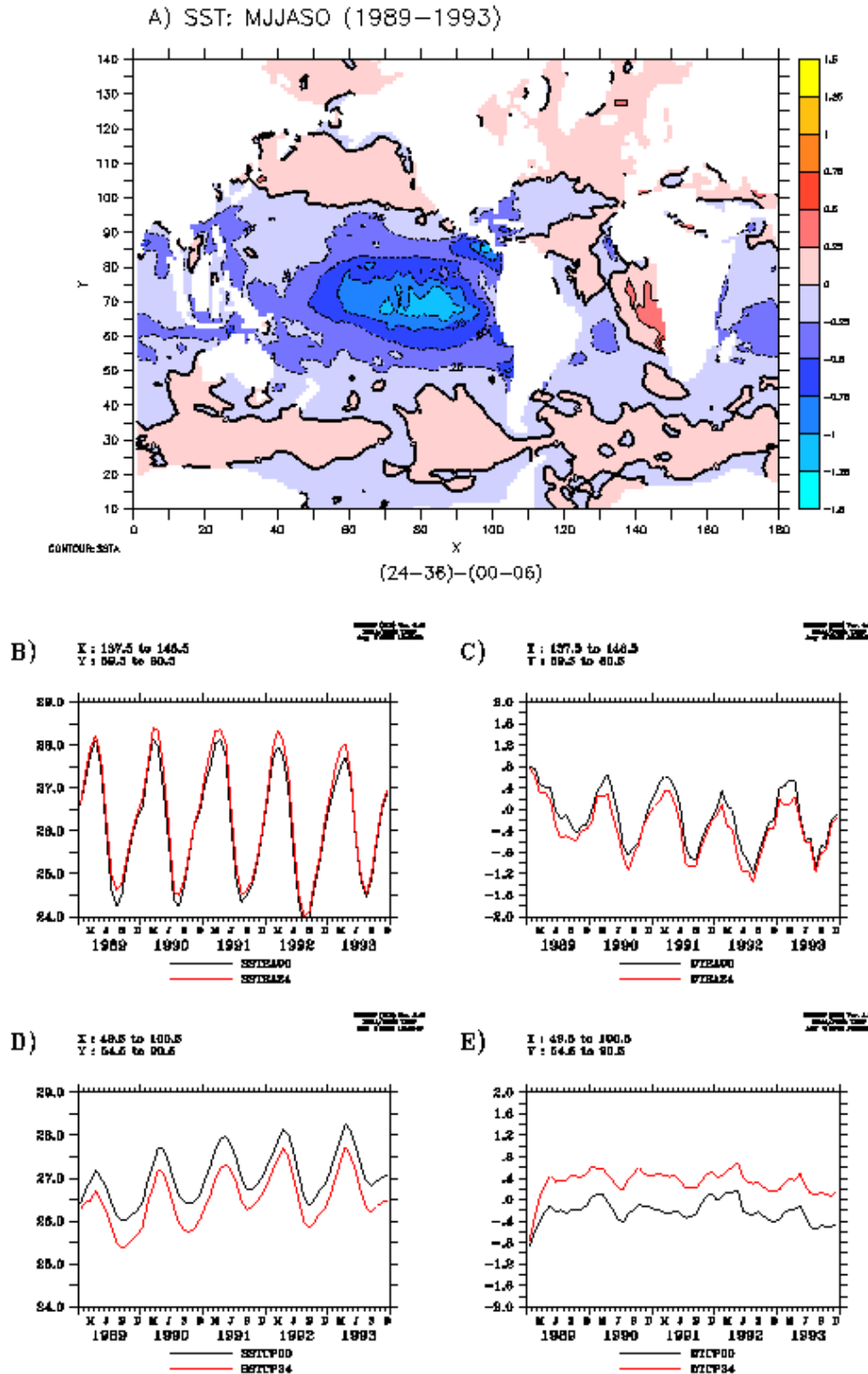


Figure 9. (a) SST ERA-40 bias between 24-36 and 0-6 hours forecast averaged from May to October (MJJASO). Comparison of 0-6 (black line) to 24-36 (red line) forcing evolutions: (b) SST and (c) relaxation term in South America off (10°N-10°S; 85°-125°E); (d) SST and (e) relaxation term in Gulf of Guinea (15°W-10°E; 5°S-10°N).

MLD was also examined (not shown). The 0-6 hr forecast is deeper than 24-30 hr forecast a central western Pacific and southwestern Indian Oceans. In these regions, averaged bias may reaches 15m. Negative bias (0-6 hr is shallower than 24-36 hr forecast) is less spread than positive bias: only southern high latitudes show bias of 10m with a maximum of the order of 30m on eastern circumpolar current (45°-55°S; 100°-110°W). The magnitude of bias in Gulf of Guinea and Central Pacific Ocean is of the order of 10% of MLD. Both regions show a seasonal variability of bias. In Gulf of Guinea bias is maximum approximately from August to October and in central Pacific Ocean during August.

6.2 ERA-40 spin-up evaluation by comparison with in-situ experiments

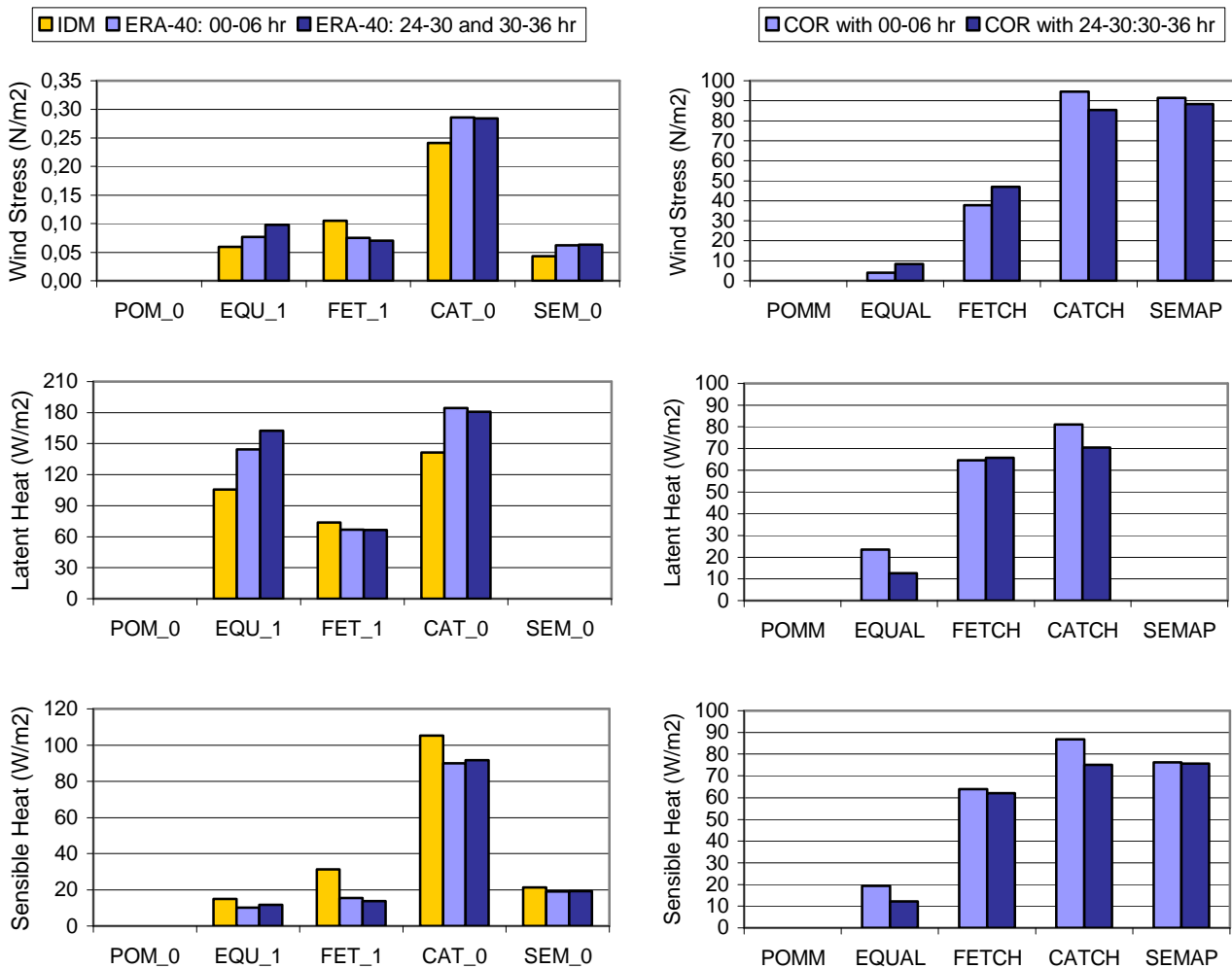


Figure 10. From top to bottom averaged wind stress, latent and sensible heat. On the left, POMME, EQUALANT FETCH, CATCH and SEMAPHORE fluxes are compared to those of ERA-40 0-6 h forecast and the combination 24-30 with 30-36 hours forecast. On the right, the correlation coefficients between in-situ experiments and ERA-40.

ERA-40 turbulent fluxes from 0-6 hr forecast and blended 24-30 with 30-36 hr forecast were compared to in-situ experiments (Figure 10). Wind stress and latent heat has generally the same behaviour: they increase with forecast distance from the initialisation time in tropical region (EQUALANT99) and remain stable in middle-latitudes. For EQUALANT99 the correlation coefficient have no statistical sense and it is impossible to conclude about the best

forecast. FETCH shows better correlation for forecasts distant from initialisation time. For CATCH and SEMAPHORE the better forecasts are those near to the initialisation time. Averaged sensible heat does not vary strongly and best correlations are for 0-6 hr forecast.

7. Conclusions

Results from the intercomparison between earlier re-analysis showed that ERA-40 has the smallest global imbalances in net air-sea surface heat fluxes. Comparison to NCEP/NCAR was made at spatial and temporal scales. ERA-40 latent heat and solar radiation is slightly larger and spatially well correlated to those of NCEP/NCAR. Sensible heat and thermal radiation are spatially badly correlated, however, generally ERA-40 thermal radiation is smaller than those of NCEP/NCAR. Correlation between interannual anomalies of heat fluxes from ERA-40 and NCEP/NCAR was examined. Interannual anomalies of sensible heat, solar radiation and net heat flux are particularly badly correlated in NH.

Comparison of ERA-40 with in-situ experiments showed that ERA-40 wind stress and latent heat are larger than in-situ experiments. Sensible heat trends are not clear. ERA-40 turbulent flux and downward solar radiation are well correlated with in-situ experiments in mean and high latitudes, however, downward solar radiation shows RMS superior to 50% of averages. Averaged ERA-40 downward thermal radiation is similar to observations.

Comparison of ERA-40 with ERA-15 in term of ocean global model showed that ERA-40 is warmer than ERA-15 in central eastern Pacific and western Atlantic. ERA-40 is particularly colder than ERA-15 in western equatorial Pacific Ocean (Central America off) whereas differences reach locally 3°C. ERA-40 mixed layer is shallower on subtropical gyre of the South Pacific and deeper in eastern Pacific than ERA-15.

ERA-40 and ERA-15 short-range forecasts were analysed as a function of spin-up, i.e. initial increase (or decrease) of model outputs with forecast length (Ramos Buarque et al., 2002, 2003). ERA-40 spin-ups were found generally smaller than those of ERA-15. This study allowed quantifying variability of fluxes related to spin-up and pointed out the most concerned areas, e.g. large latent heat spin-ups were observed particularly in tropical regions. In continuity, ERA-40 turbulent fluxes from 0-6 hr forecast and blended forecasts from 24-30 and 30-36 hr were compared to in-situ experiments. Results showed that wind stress and latent heat increase with the range from the initialisation time in tropical region and remain almost stable in middle-latitudes. In some cases (CATCH and SEMAPHORE) fluxes from 0-6 hr forecast are better correlated to observations. In this case, analysed fields were not balanced in the way of the model's physics. Comparison of global ocean model response to ERA-40 air-sea surface fluxes spin-up was also examined. In the central eastern tropical Pacific the SST from 0-6 hr forecast is locally 1.5°C warmer than those of 24-36 hr forecast. Gulf of Guinea shows seasonal bias of SST: 0-6 hr is locally 1°C colder than 24-36 hr forecast during February-March-April and July-August-September. This result raises the question: What is the response of a coupled ocean/atmosphere model vis-à-vis of seasonal biased heat and momentum fluxes? Will be the seasonal bias of heat and momentum amplified or not?

Acknowledgements. We would like thanking the members of the MERCATOR Project their commitment. We would especially like to thank Nicolas FERRY for his technical support and Laurence FLEURY who was promptly answered our request providing the ocean model.

References

- Barnier, B., 1998. Forcing the ocean. *Ocean Modelling and Parameterization*. E.P. Chassignet and J. Verron (eds.) Kluwer Academic Publishers, The Netherlands. 45-80.
- Beljaars, A. and P. Källberg, 2001. Ocean Fluxes in the ECMWF 40-Year Re-analysis (ERA-40). Proceedings of the WCRP/SCOR Workshop on Intercomparison and Validation of Ocean-Atmosphere Flux Fields, 21-24 May 2001 (Bolger Center, Potomac, MD, USA). WCRP-115, WMO/TD-N° 1083: 18-20.
- Bonekamp, H., A. Sterl and G.J. Komen, 1999. Interannual variability in the Southern Ocean from an ocean model forced by European Centre for Medium-Range Weather Forecasts reanalysis fluxes. *Journal of Geophysical Research*. Vol. 104, No. C6: 13317-13331.
- Brut, A., 2002. Mesures des échanges surface-atmosphère: Paramétrisation des flux sur l'océan et mise au point d'un instrument pour la détermination de flux d'espèce en trace. Thèse de Doctorat de l'Université Paul Sabatier. Centre National de Recherches Météorologiques, 42 avenue Coriolis, 31057 Toulouse Cedex 1, France. 207pp.
- Dupuis H., C. Guérin, A. Weill, D. Hauser, 1999. Heat fluxes by the inertial dissipation method during FETCH, Proceedings (with referees) of the Symposium on the wind-driven Air-Sea Interface, Sydney, School of Mathematics, University of New South Wales, Sydney, Australia, M. Banner Ed., 11-15 January, 297-304.
- Eymard, L., S. Planton, P. Durand, Y. Camus, P.Y. Le Traon, L. Prieur, A. Weill, D. Hauser, B. Le Squire, J. Rolland, J. Pelon, F. Baudin, B. Benech, J.L. Brenguier, G. Caniaux, P. De Mey, E. Dombrowski, A. Druilhet, H. Dupuis, B. Ferret, C. Flamant, P. Flamant, F. Hernandez, D. Jourdan, K.B. Katsaros, D. Lambert, J.M. Lefevre, P. Le Borgne, A. Marsouin, H. Roquet, J. Tournadre, V. Trouillet, B. Zakardjian, 1996. Study of the air-sea interactions at the mesoscale, the SEMAPHORE experiment. *Ann. Geophys.*, Vol. 14, 986-1015
- Eymard, L., G. Caniaux, H. Dupuis, L. Prieur, H. Giordani, R. Trodec, P. Bessemoulin, G. Lachaud, G. Bouhours, D. Bourras, C. Guérin, P. Le Borgne, A. Brisson and A. Marsouin, 1999. Surface fluxes in the North Atlantic current during CATCH/FASTEX, *Quart. J. Roy. Meteor. Soc.*, Vol. 125, 3563-3599.
- Eymard, L., S. Planton, P. Durand, Y. Camus, P.Y. Le Traon, L. Prieur, A. Weill, D. Hauser, B. Le Squire, J. Rolland, J. Pelon, F. Baudin, B. Benech, J.L. Brenguier, G. Caniaux, P. De Mey, E. Dombrowski, A. Druilhet, H. Dupuis, B. Ferret, C. Flamant, P. Flamant, F. Hernandez, D. Jourdan, K.B. Katsaros, D. Lambert, J.M. Lefevre, P. Le Borgne, A. Marsouin, H. Roquet, J. Tournadre, V. Trouillet, B. Zakardjian, 1996. Study of the air-sea interactions at the mesoscale, the SEMAPHORE experiment. *Ann. Geophys.*, Vol. 14, 986-1015.
- Ferry, Nicolas 2001. Flux de Surface de Chaleur et d'Eau Douce en Atlantic Nord: contributions aux variations de niveau de mer et apports pour la modélisation numérique océanique. Thèse de Doctorat de l'Université Paul Sabatier. Laboratoire d'Etudes en Géophysique et Océanographie Spatiales (UMR 5566). 14, Av. Edouard Belin, 31400 Toulouse France. 214
- Giordani, H., S. Planton, B. Benech and B.-H. Kwon, 1998. Atmospheric boundary Layer response to sea surface temperatures during the SEMAPHORE experiment, *Journal of Geophysical Research*, Vol. 103, No. C11, 25,047-25,060.
- Giordani, Hervé and Serge Planton, 2000. Modeling and Analysis of Ageostrophic Circulation over the Azores Oceanic Front during the SEMAPHORE Experiment. *Monthly Weather Review*. Vol. 128, No. 7: 2270-2287.
- Gibson, J. K., P. Källberg, S.Uppala, A. Hernandez, A. Nomura and E. Serrano, 1999. ECMWF Re-Analysis Project Report Series, 1. ERA-15 Description (Version 2 – January 1999), 73p.
- Kalnay, E., M. Kanamitsu, R. Kistler, W. Collins, D. Deaven, L. Gandin, M. Iredell, S. Saha, G. White, J. Woollen, Y. Zhu, A. Leetmaa, B. Reynolds, M. Chelliah, W. Ebisuzaki, W. Higgins, J. Janowiak, K.C. Mo, C. Ropelewski, J. Wang, R. Jenne and D. Joseph, 1996. The NCEP/NCAR 40-Year Reanalysis Project. *Bulletin of the American Meteorological Society*. Vol. 77, No. 3: 437-472.
- Kistler, R., E. Kalnay, W. Collins, S. Saha, G. White, J. Woollen, M. Chelliah, W. Ebisuzaki, M. Kanamitsu, V. Kousky, H. van den Dool, R. Jenne and M. Fiorino, 2001. The NCEP-NCAR 50-Year Reanalysis. *Monthly Means CD-ROM and Documentation*. *Bulletin of the American Meteorological Society*. Vol. 82, No. 2: 247-268.

- Monterey, G., and S. Levitus, 1997: Seasonal variability of mixed layer depth for the World Ocean. NOAA Atlas, NESDIS 14, 100, Washington, D.C.
- Ramos Buarque, S., Giordani H., Caniaux G. and Planton S., 2003. Evaluation of the ERA-40 Air-Sea Surface Heat Flux Spin-up. *Dynamics of Atmospheres and Oceans* (accepted).
- Ramos Buarque, S., Giordani H., Caniaux G. and Planton S., 2002: ERA-40 Ocean Surface Heat Flux: Model Spins Evaluation. *Atelier de Modélisation de l'Atmosphère, CNRM, Toulouse, France, 17-19 décembre*, 121-124.
- Reynolds, R., and T. Smith, 1994. Improved global sea surface temperature analyses using optimum interpolation. *J. Climate*, 7, 929–948
- Schubert, Siegfried D., Richard B. Rood, James Pfaendner, 1993. An Assimilated Dataset for Earth Science Applications. *Bulletin of the American Meteorological Society*. Vol. 74, No. 12: 2331-2342.
- Weill, A., L. Eymard, G. Caniaux, D. Hauser, S. Planton, H. Dupuis, A. Brut, C. Guerin, P. Nacass, A. Butet, S. Cloché, R. Pedreros, P. Durand, D. Bourras, H. Giordani, G. Lachaud, and G. Bouhours, 2003. Toward a Better Determination of Turbulent Air-Sea Fluxes from Several Experiments. *J. Climate*, 16, 600–618.
- White, G. and S. Saha, 1999. Estimation of the global energy and water cycle from global data assimilation. *Global Energy and Water Cycles*. K. A. Browning and R. J. Gurney, Cambridge University Press, Cambridge, UK, 55-60.
- White, G. 2001. Air-Sea Fluxes from Data Assimilation for Numerical Weather Prediction. *Proceedings of the WCRP/SCOR Workshop on Intercomparison and Validation of Ocean-Atmosphere Flux Fields, 21-24 May 2001* (Bolger Center, Potomac, MD, USA). WCRP-115, WMO/TD-N° 1083: 14-17.
- Uppala, S., J.K. Gibson, M. Fiorino, A. Hernandez, P. Kållberg, Xu Li, K. Onogi and S. Saarinen, 2000. *Proceedings of the Second WCRP International Conference on Reanalyses, 23-27 August 1999* (Wokefield Park, Reading, UK). WCRP-109, WMO/TD-N° 985: 9-13.